ANZIAM J. 51(2010), 406–415
doi:10.1017/S144618111000091X

A NOTE ON APPROXIMATE BENCHMARK SOLUTIONS FOR VISCOUS TWO-LAYER FLOWS

M. SELLIER[✉1] and R. D. LENZ[2]

(Received 21 December, 2009; revised 25 October, 2010)

Abstract

An important test of the quality of numerical methods developed to track the interface between two fluids is their ability to reproduce test cases or benchmarks. However, benchmark solutions are scarce and virtually nonexistent for complex geometries. We propose a simple method to generate benchmark solutions in the context of the two-layer flow problem, a classical multiphase flow problem. The solutions are obtained by considering the inverse problem of finding the required channel geometry to obtain a prescribed interface profile. This viewpoint shift transforms the problem from that of having to solve a complex differential equation to the much easier one of finding the roots of a quartic polynomial.

2000 *Mathematics subject classification*: primary 76T99; secondary 65L09.

Keywords and phrases: multiphase flow, long wave approximation, exact solution.

1. Introduction

The flow of two immiscible fluid layers in channels appears in a range of applications such as lubricated piping, oil recovery, and lithographic printing [7]. Such flows are also common in microfluidic technologies [16]. Beyond the mere technological interest, such flows epitomise one of the great challenges of modern fluid dynamics research, that is, modelling the dynamics of interfaces in multiphase flows. This field is rich in available literature and a survey is beyond the scope of this paper; the interested reader is referred to the review of Scardovelli and Zaleski [14], for example.

Alongside the development of analytical and numerical techniques to solve such flows, it is essential to establish a library of benchmark solutions which can be used to validate the results obtained. The complexity and nonlinearity of the Navier–Stokes equations with the required boundary conditions strongly limit the availability of such solutions, even more so in nontrivial geometries. In this paper, we propose a simple

[1]Department of Mechanical Engineering, The University of Canterbury, Private Bag 4800, Christchurch 8140, New Zealand; e-mail: mathieu.sellier@canterbury.ac.nz.
[2]ExxonMobil Research and Engineering, Fairfax, VA 22037, USA; e-mail: richard.d.lenz@gmail.com.

technique to build solutions for the two-layer flow problem in corrugated channels. It is based on the analysis of Lenz and Kumar [7] who reduced the Navier–Stokes equations to a nonlinear ordinary differential equation for the interface profile in the long-wave approximation limit. This flow configuration is particularly suitable as a benchmark problem as the interaction between the wall topography and the two-fluid layer interface is nontrivial, as recently demonstrated by Luo and Pozrikidis [9] and Luo *et al.* [8].

The main idea behind the construction of the benchmark solutions is to adopt a reverse stand whereby the interface between the two fluids is a prescribed function and the corresponding corrugation profile is sought. This viewpoint shift transforms the problem from that of having to solve a complex nonlinear differential equation to that of finding the roots of a quartic polynomial. This approach offers some advantages:

- The approach does not require the discretization of the governing ordinary differential equation, so the solutions generated are free of discretization error. Moreover, the solutions to the ordinary differential equation are exact.
- The implementation is significantly simplified since finding the roots of a polynomial is routine practice compared to discretizing and solving a nonlinear ordinary differential equation or indeed the full Navier–Stokes equations.
- The existence (or not) of a solution to the polynomial provides an indication of the admissibility of an interface profile.

The concept of generating a class of solutions for a given prescribed interface profile was first introduced by Sautreaux towards the end of the nineteenth century in the context of steady, inviscid, and irrotational free-surface flows [13]. The idea was subsequently exploited by Rudzki [12] and Richardson [11] to compute exact solutions of free-surface flows over a corrugated bottom. More than a century later, the technique was extended by MacDonald *et al.* [10] to find closed-form solutions of open-channel flows. Tuck [17] also built on the work of Sautreaux to compute exact solutions of the flow of air over free surfaces of stationary water. Following a similar tack, Hocking [4] derived exact solutions of problems involving a line source or sink beneath a cusped free surface. Finally, Sellier [15] used a similar procedure to find which substrate profile leads to a desired or observed free-surface shape in the context of thin film flows over corrugations. Viscous effects play an important role in the latter study as in the present case.

The next section gives a brief description of the problem and governing equations. It is followed by a description of the idea behind the derivation of the solutions to the problem, and a demonstration of the validity of the method. Finally, the limitations of the proposed technique are discussed and conclusions drawn.

2. Problem definition and governing equations

Figure 1 illustrates the problem considered and the notation adopted. The flow is in the positive x-direction and is driven either by an applied pressure gradient $\Delta P/L$ or the motion of the upper boundary with velocity u_T. This corresponds to

https://doi.org/10.1017/S144618111000091X Published online by Cambridge University Press

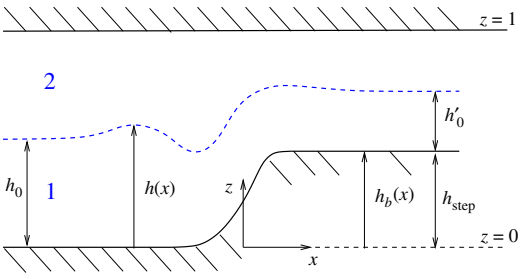

FIGURE 1. Sketch of the problem considered and the notation adopted (following Lenz and Kumar [7]).

the Poiseuille or Couette flow configuration, respectively. The fluids, labelled 1 and 2, are incompressible, Newtonian, immiscible and form two layers. The viscosities of fluids 1 and 2 are μ_1 and μ_2, respectively, and the corresponding densities are ρ_1 and ρ_2. The height of the lower boundary is $h_b(x)$, while that of the interface between fluids 1 and 2 is $h(x)$. The asymptotic values of the interfacial height are h_0 upstream and $h_{\text{step}} + h_0'$ downstream.

In this paper we present what could be termed the "base case" in which the viscosity ratio μ_r and the density ratio ρ_r are set equal to 1. The significance of this limit is that it creates an equal contribution from both layers. In the limit in which these ratios approach zero, the well-studied case of a single fluid layer flowing over topography is obtained. As discussed in [7], this causes the size of capillary features to be substantially larger than in the two-layer case. On the other hand, increases in μ_r and ρ_r cause the top layer to dominate the flow, such that the impact of topography on the fluid interface is less significant. Obviously, increases in ρ_r would also lead to an instability associated with density stratification, which is not incorporated into our formulation. Attention is therefore focused on the "base case", having an understanding already in place of how variation in the density and viscosity parameters would impact the problem's physics. A complete derivation of the equation governing the interfacial height follows, but the interested reader is referred to [6, 7] for further details.

The vertical length scale of the problem is taken to be the height of the wide part of the channel. This dimensional (indicated by the tilde) thickness is $\tilde{h}_t$, and in accordance with lubrication theory is assumed to be much smaller than $\tilde{l}$, the length scale of variations in the x-direction. A small parameter $\epsilon = \tilde{h}_t/\tilde{l}$ is defined, which leads to the following scaling for the dimensionless lengths and velocities:

$$x = \frac{\epsilon \tilde{x}}{\tilde{h}_t}, \quad z = \frac{\tilde{z}}{\tilde{h}_t}, \quad u_i = \frac{\tilde{u}_i}{\tilde{u}_\circ}, \quad w_i = \frac{\tilde{w}_i}{\epsilon \tilde{u}_\circ}.$$

The subscript i indicates to which fluid phase a variable corresponds, and u and w are the fluid velocities in the x and z directions. The horizontal velocity scale is $\tilde{u}_\circ = \mu_1/(\rho_1 \tilde{h}_t)$, where μ_1 and ρ_1 are the viscosity and density of the lower layer.

https://doi.org/10.1017/S144618111000091X Published online by Cambridge University Press

The scalings for the dimensionless time and pressure variables are then

$$t = \frac{\epsilon \tilde{t}\tilde{u}_\circ}{\tilde{h}_t}, \qquad p_i = \frac{\epsilon \tilde{p}_i \tilde{h}_t}{\mu_1 \tilde{u}_\circ}.$$

Development of the governing equations begins with the dimensional momentum balance and stress balance at the fluid interface:

$$\rho_i(\partial_{\tilde{t}}\tilde{\mathbf{u}}_i + \tilde{\mathbf{u}}_i \cdot \nabla\tilde{\mathbf{u}}_i) = -\nabla\tilde{p}_i + \rho_i \mathbf{g} + \mu_i \nabla^2\tilde{\mathbf{u}}_i, \tag{2.1}$$

$$\mathbf{T}_1 \cdot \mathbf{n} - \mathbf{T}_2 \cdot \mathbf{n} = -\kappa\tilde{\gamma}\mathbf{n}, \tag{2.2}$$

where $\tilde{\mathbf{u}}_i$ is the velocity vector in fluid i, $\mathbf{T}_i$ is the stress tensor in fluid i, $\mathbf{g}$ is the gravity vector, $\mathbf{n}$ is the vector normal to the fluid interface pointing into fluid 2, κ is the interfacial curvature, and $\tilde{\gamma}$ is the dimensional interfacial tension. The set of lubrication equations is obtained by substituting the dimensionless variables into (2.1) and (2.2) and discarding terms of order ϵ and smaller. The momentum balance becomes

$$\begin{aligned} 0 &= -\partial_x p_i + \frac{\rho_i}{\rho_1} B + \frac{\mu_i}{\mu_1}\partial_z^2 u_i, \\ 0 &= \partial_z p_i, \end{aligned} \tag{2.3}$$

where $B = \tilde{h}_t^2 \rho_1 g_x/(\mu_1 \tilde{u}_\circ)$ is the dimensionless horizontally acting body force. The normal and shear stress balances are also simplified:

$$\begin{aligned} 3\mathrm{Ca}^{-1}\partial_x^2 h &= p_2 - p_1, \\ \mu_r \partial_z u_2 &= \partial_z u_1. \end{aligned} \tag{2.4}$$

Here μ_r is the viscosity ratio, μ_2/μ_1, and Ca^{-1} is the inverse capillary number:

$$\mathrm{Ca}^{-1} = \frac{\epsilon^3 \tilde{\gamma}}{3\mu_1 \tilde{u}_\circ}.$$

The ϵ^3 term is included to keep capillary forces in balance with viscous forces.

Velocity profiles may be obtained by integrating (2.3) for both fluid layers and applying no-slip boundary conditions at the channel walls, and velocity and shear stress continuity at the fluid interface. After doing so, the only unknowns in the problem are the pressure gradients, $\partial_x p_i$, and the interfacial height, h. The three equations needed to determine these unknowns are the normal stress balance, and mass conservation for both fluid layers in the form of constant flow-rate conditions. To employ mass conservation we first calculate the base flow-rates for each fluid layer where the fluid interface is flat in the wide part of the channel:

$$Q_1 = -\frac{\Delta P/L - B}{12(1+h_r)^3} + \frac{u_I^{\mathrm{base}}}{2(1+h_r)}, \tag{2.5}$$

$$Q_2 = -\frac{(\Delta P/L - \rho_r B)h_r^3}{12\mu_r(1+h_r)^3} + \frac{h_r(u_I^{\mathrm{base}} + u_T)}{2(1+h_r)}, \tag{2.6}$$

https://doi.org/10.1017/S144618111000091X Published online by Cambridge University Press

with the base interfacial velocity, u_I^{base}, given by:

$$u_I^{\text{base}} = -\frac{[\Delta P/L - B(h_r\rho_r + 1)/(1 + h_r)]hr}{2(\mu_r + h_r)(1 + h_r)} + \frac{\mu_r u_T}{\mu_r + h_r}.$$

In these equations h_r is the height ratio, $(1 - h_\circ)/h_\circ$, and ρ_r is the density ratio, ρ_2/ρ_1.

The velocity profiles in each layer as a function of x are integrated with respect to z and equated to (2.5) and (2.6) to yield the two constant flow-rate condition equations needed to solve for $\partial_x p_i$:

$$\int_{h_b}^{h} u_1\, dz = (-\partial_x p_1 + B)\frac{(h - h_b)^3}{12} + u_I\frac{h - h_b}{2} = Q_1,$$
$$\int_{h}^{1} u_2\, dz = (-\partial_x p_2 + \rho_r B)\frac{(1 - h)^3}{12\mu_r} + (u_T + u_I)\frac{1 - h}{2} = Q_2.$$

Here h, h_b, u_I, and both $\partial_x p_i$ are all functions of x, and the expression for the interfacial velocity as a function of position is

$$u_I = \frac{1 - h}{2(r + \mu_r)}[(-\partial_x p_1 + B)(h - h_b) + (-\partial_x p_2 + \rho_r B)(1 - h)] + \frac{\mu_r u_T}{r + \mu_r},$$

where r is a local height ratio, $(1 - h)/(h - h_b)$. The resulting expressions for $\partial_x p_i$ are then substituted into the differentiated form of (2.4) to produce the governing equation for h:

$$3\text{Ca}^{-1}\partial_x^3 h = [Q_1 C_1 + Q_2 C_2 + u_T C_3]/C_4 + (\rho_r - 1)B, \tag{2.7}$$

where

$$\begin{aligned} C_1 &= r^2(3r^2 + 12\mu_r r + 9\mu_r), \\ C_2 &= -\mu_r(9r^2 + 12r + 3\mu_r), \\ C_3 &= \mu_r(1 - h)(3r^2 + 6r + 3\mu_r), \\ C_4 &= (1 - h)^3(r + \mu_r). \end{aligned} \tag{2.8}$$

Equation (2.7) is a third-order ordinary differential equation for the unknown function $h(x)$. It can be solved to obtain the steady-state profile of the interface as a function of the various parameters. This equation is solved using the FORTRAN code developed by Lenz [6]. The equation was discretized using finite differences, the third-order derivative being calculated using a centered-difference formula with second-order error.

For illustration purposes, Figure 2 shows the response of the interface between the two fluids to a step-up or a step-down in the lower boundary. For this particular case, $\Delta P/L$ and u_T are set to zero, the capillary number is equal to 1 and $B = 12$. Both the density and viscosity ratios are set to unity. These conditions are used for the remainder

https://doi.org/10.1017/S144618111000091X Published online by Cambridge University Press

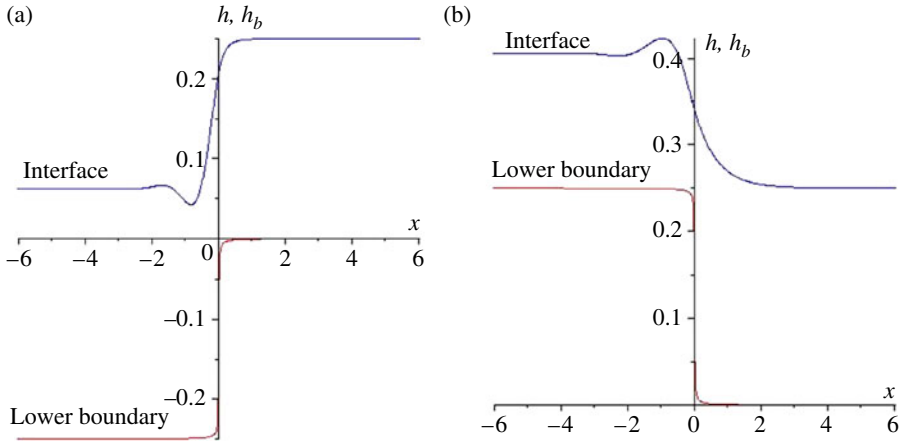

FIGURE 2. Sample result for (a) a step-up and (b) a step-down.

of the paper but are not restrictive since the method described in the following section applies indiscriminately. The step in the lower boundary is introduced by using an arctangent function, which ensures that it is continuously differentiable, according to

$$h_b(x) = h_{\text{step}}\left(\frac{1}{2} \pm \frac{1}{\pi}\arctan\left(\frac{x}{\delta}\right)\right),$$

where the $\pm$ is "+" for a step-up and "−" for a step-down, and δ is the horizontal length scale for topography changes. The value of δ dictates the steepness of the step and is set to 0.31 in the present case. The size of the step h_{step} is equal to 0.25.

The interface shows a number of features reminiscent of the flow of solitary thin fluid films over steps as investigated in [2, 3]. Indeed, a depression can be observed ahead of the step-down and a ridge ahead of the step-up. These are preceded by a series of interface oscillations, resulting from a competition between the substrate tending to impress its topography on the interface simply as a result of mass conservation, and interfacial tension tending to flatten the interface [5].

3. Derivation of benchmark solutions

The question we are trying to address is: can we easily produce solutions of (2.7) and (2.8) that could be used as a benchmark to assess the validity of interface-tracking algorithms in nontrivial geometries? Because of the limitations inherent to the model described here, the solutions produced will only be valid and therefore useful as benchmark solutions in the inertialess regime and for gently sloped interfaces. In order to address this question, we consider the inverse problem of finding the required bottom profile which yields a prescribed interface profile. We will show that by shifting the viewpoint from the direct to the inverse formulation, we actually transform

https://doi.org/10.1017/S144618111000091X Published online by Cambridge University Press

the problem from solving a highly nonlinear ordinary differential equation to finding the root of a quartic polynomial.

Assuming that the interface between the two fluids is prescribed and given by $h(x) = h_p(x)$, (2.7) and (2.8) can be recast in the form of the quartic polynomial

$$A_4 r^4 + A_3 r^3 + A_2 r^2 + A_1 r + A_0 = 0,$$

where the coefficients A_i are given by

$$\begin{aligned}
A_4 &= 3Q_1,\\
A_3 &= 12\mu_r Q_1,\\
A_2 &= 9\mu_r(Q_1 - Q_2) + 3u_T\mu_r(1 - h_p),\\
A_1 &= -\frac{3}{\mathrm{Ca}}(1 - h_p^3)\frac{d^3h_p}{dx^3} - 12\mu_r Q_2 + 6u_T\mu_r(1 - h_p) + (\rho_r - 1)B(1 - h_p^3),\\
A_0 &= \frac{3}{\mathrm{Ca}}(1 - h_p^3)\mu_r\frac{d^3h_p}{dx^3} - 3\mu_r^2 Q_2 + 3\mu_r^2 u_T(1 - h_p) + (\rho_r - 1)B(1 - h_p^3)\mu_r.
\end{aligned} \tag{3.1}$$

For a known interface profile, the coefficients of this quartic polynomial are defined for all x. It is possible to find a closed-form expression for the roots of a quartic polynomial using the method due to Ferrari (see [1], for example) but it is preferred here to simply use the Maple function *solve*. A remarkable fact is that, of the four possible roots, the one of interest is always the one with the smallest value. Once the value of r is identified, the height of the lower boundary is simply retrieved according to $h_b(x) = (h_p(x)(r(x) + 1) - 1)/r(x)$. The pair of functions $(h_b(x), h_p(x))$ is a solution of the ordinary differential equation (2.7).

4. Illustrative examples

In order to assess the idea presented in the previous section, a range of prescribed interface profiles was tested. Obviously, an interface profile needs to be at least three times differentiable for the coefficients in (3.1) to be defined. The profiles considered were defined in terms of the hyperbolic tangent function or the exponential function as follows:

$$h_p^{\tanh}(x) = h_0 + \frac{h_0'}{2}\left(1 + \tanh\left(\frac{x - x_0}{\delta}\right)\right), \tag{4.1}$$

$$h_p^{\exp}(x) = h_0 + h_0' \exp\left(-\left(\frac{x - x_0}{\delta}\right)^2\right). \tag{4.2}$$

Figure 3 illustrates the required bottom profile $h_b(x)$ which results in an interface defined by (4.1) with $h_0 = 0.5$, $h_0' = 0.25$ and $\delta = 0.3$. The bottom profile is peculiar with an initial slow increase followed by a plateau and a region of steeper increase. Similarly, Figure 4 shows the bottom profile and corresponding fluid interface

https://doi.org/10.1017/S144618111000091X Published online by Cambridge University Press

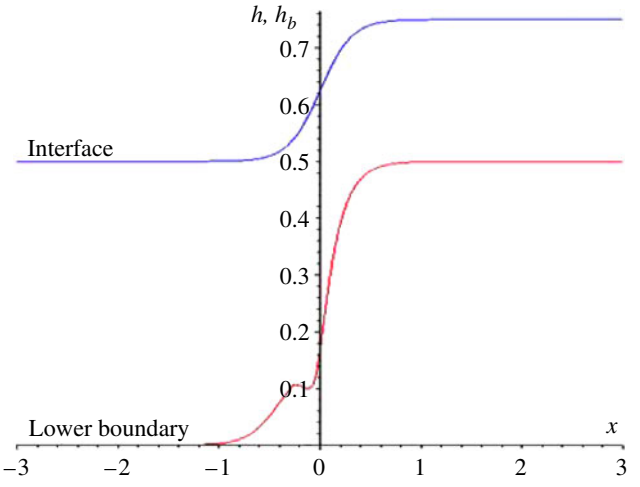

FIGURE 3. The computed bottom boundary (lower curve) required to obtain the interface profile defined by the hyperbolic tangent function (4.1) with $h_0 = 0.5$, $x_0 = 0$, $h_0' = 0.25$ and $\delta = 0.3$ (upper curve).

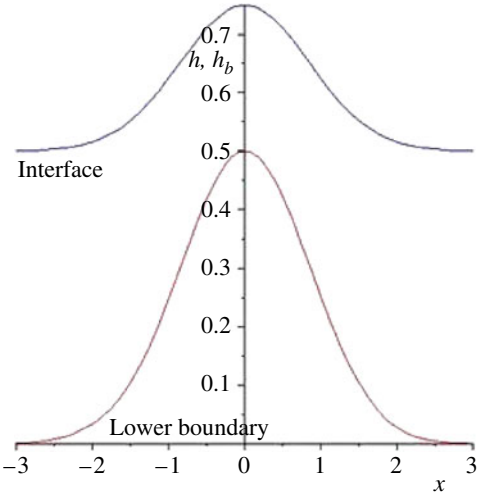

FIGURE 4. The computed bottom boundary (lower curve) required to obtain the interface profile defined by the exponential function (4.2) with $h_0 = 0.5$, $x_0 = 0$, $h_0' = 0.25$ and $\delta = 1.2$ (upper curve).

prescribed by (4.2) with $h_0 = 0.5$, $x_0 = 0$, $h_0' = 0.25$ and $\delta = 1.2$. In both cases, the validity of the approach was confirmed by using the derived bottom profile as an input to the FORTRAN code which solves (2.7) and (2.8), and comparing the computed interface to the one given by (4.1) and (4.2). The profiles were indistinguishable.

Besides providing a simple way to build solutions to the two-layer flow problem, the analysis above also gives information on the existence of solutions. Indeed, as one

https://doi.org/10.1017/S144618111000091X Published online by Cambridge University Press

would expect, there exists a limit to how distorted the interface between two fluids can become: interface tension restricts how rapidly the interface height can vary. For example, as δ becomes smaller in (4.1), the interface varies between h_0 and $h_0 + h_0'$ over a shorter distance, and one would expect the solution to cease to exist as δ tends to zero, since the physical requirement $(h - h_b) > 0$ is no longer met. This is indeed observed. For a step-down the critical value below which a physical solution ceased to exist lay between 0.4 and 0.45, while for a step-up it lay between 0.25 and 0.3. This result implies an unexpected asymmetry between the step-up and the step-down, that is, the interface is able to "take" a step-up over a shorter distance than a step-down.

5. Concluding remarks

This paper describes a simple way to generate solutions to the two-layer flow problem. It is based on an ordinary differential equation introduced by Lenz and Kumar [7]. The solutions are simply generated by considering the inverse problem of fixing the interface profile and seeking the required bottom profile. In doing so, the problem is transformed from one of having to solve a highly nonlinear differential equation to finding the roots of a quartic polynomial. The solutions found using this strategy are exact in the sense that they are free of discretization error. The validity of the proposed approach is demonstrated on two examples but an infinite number of solutions can be built, in principle. Validity is only justified within the limits of the chosen approximation. The most obvious one is the "long-wave" approximation which requires the amplitude of the interface variations to be much smaller than the characteristic wave length ($\epsilon \ll 1$). This restriction is, however, not too severe if the benchmark solutions are used for validation purposes.

Acknowledgements

The authors would like to thank the reviewers for providing useful references. The help of Emmanuel Trelluyer, summer intern at the University of Canterbury, is also gratefully acknowledged.

References

[1] M. Abramowitz and I. A. Stegun (eds), *Handbook of mathematical functions with formulas, graphs, and mathematical tables*, 9th printing (Dover, New York, 1972).

[2] M. M. J. Decré and J. C. Baret, "Gravity-driven flows of viscous liquids over two-dimensional topographies", *J. Fluid Mech.* **487** (2003) 147–166.

[3] P. H. Gaskell, P. K. Jimack, M. Sellier, H. M. Thompson and M. C. T. Wilson, "Gravity-driven flow of continuous thin liquid films on non-porous substrates with topography", *J. Fluid Mech.* **509** (2004) 253–280.

[4] G. C. Hocking, "Cusp-like free surface flows due to a submerged source or sink in the presence of a flat or sloping bottom", *J. Aust. Math. Soc. Ser. B* **26** (1985) 470–486.

[5] S. Kalliadasis, C. Bielarz and G. M. Homsy, "Steady free-surface thin film flows over topography", *Phys. Fluids* **12** (2000) 1889–1898.

[6] R. D. Lenz, Liquid displacement in lithographic printing: modeling and visualization, Ph. D. Thesis, University of Minnesota, 2007.

[7] R. D. Lenz and S. Kumar, "Steady two-layer flow in a topographically patterned channel", *Phys. Fluids* **19** (2007) 102103.
[8] H. Luo, M. G. Blyth and C. Pozrikidis, "Two-layer flow in a corrugated channel", *J. Engrg. Math.* **60** (2008) 127–147.
[9] H. Luo and C. Pozrikidis, "Shear-driven and channel flow of a liquid film over a corrugated or indented wall", *J. Fluid Mech.* **556** (2006) 167–188.
[10] I. MacDonald, M. J. Baines, N. K. Nichols and P. G. Samuels, "Analytic benchmark solutions for open-channel flows", *J. Hyd. Eng.* **123** (1997) 1041–1045.
[11] A. R. Richardson, "Stationary waves in water", *Phil. Mag.* **40** (1920) 97–110.
[12] M. P. Rudzki, "Über eine Klasse hydrodynamischer Probleme mit besonderen Grenzbedingungen", *Math. Ann.* **50** (1898) 269–281.
[13] C. Sautreaux, "Sur une question d'hydrodynamique", *Ann. Sci. Éc. Norm. Super.* **10** (1893) S.95–S.182.
[14] R. Scardovelli and S. Zaleski, "Direct numerical simulation of free-surface and interfacial flow", *Annu. Rev. Fluid Mech.* **31** (1999) 567–603.
[15] M. Sellier, "Substrate design or reconstruction from free surface data for thin film flows", *Phys. Fluids* **20** (2008) art:062106.
[16] T. M. Squires and S. R. Quake, "Microfluidics: fluid physics at the nano-liter scale", *Rev. Mod. Phys.* **77** (2005) 977–1026.
[17] E. O. Tuck, "On air flow over free surfaces of stationary water", *J. Aust. Math. Soc. Ser. B* **19** (1975) 66–80.

https://doi.org/10.1017/S144618111000091X Published online by Cambridge University Press